Paper II

The C1s photoelectron spectrum of ethanol: Franck-Condon transitions in a system with large-amplitude anharmonic vibrations coupled to a harmonic-oscillator bath.

M. Abu-samha and K. J. Børve

Department of Chemistry, University of Bergen, NO-5007 Bergen, Norway

(Dated: August 30, 2006)

Ethanol exists in two conformations, *anti* and *gauche*. When *gauche*-ethanol is core-ionized at the methyl carbon, strong repulsion between the hydroxyl proton and the ionized methyl group leads to a change in conformation, from *gauche* to *anti*. Franck-Condon analysis based on the harmonic oscillator approximation is not able to describe well the nuclear dynamics accompanying the electronic event. A vibrational adiabatic approach to Franck-Condon analysis of systems with a few highly displaced oscillators coupled to a bath of harmonic oscillators is presented in a general way. The theory is subsequently applied to the lineshape of the carbon 1s photoelectron spectrum of ethanol, with very good results.

I. INTRODUCTION

Nuclear dynamics following a primary electronic excitation or ionization event is a rich source of information about the initial and final electronic states involved in the process. This has been known for a long time for valence spectroscopies such as ultraviolet and visible absorption spectroscopy (UV-vis), ultraviolet photoelectron spectroscopy (UPS), fluorescence spectroscopy and others. [1] Recently and thanks to the technical development of third generation synchrotrons and high-resolution electron spectrometers, x-ray absorption and photoelectron spectroscopies have reached a state where the fine-structure in these spectra can be used to explore the nuclear dynamics following ionization.

Theory has proven an indispensible tool for extracting information about molecular structure, vibrational modes and force constants from the lineshape or vibrational fine structure in the electronic spectra. The accepted standard for this kind of calculations is the Franck-Condon principle in conjunction with the harmonic oscillator approximation for the vibrational states. This requires optimization of the molecular structure of the initial and final states involved in the electronic transition, as well calculation of force-constant matrices (Hessian) for both states. This can be done routinely for the electronic ground state and goes from routine to very difficult depending on the complexity of the electronic final state. In our work on core-ionized molecules, [2–5] we have been able to simplify the electronic problem by representing the ionized core by an effective core potential. This makes it possible to address the ionized final state with the same ease as the electronic ground state.

While the harmonic model is extremely useful, anharmonic effects are readily seen in the spacing or relative intensities in vibrational progressions in well-resolved spectra. This is interesting in its own right, and for small molecules anharmonicity may be quantitatively accounted for in the theoretical model. If the electronic final state is dissociative, the vibrational envelope becomes broad and featureless. While providing proof for dissociation, the lack of structure in the band makes a detailed analysis of the anharmonicity of the potential energy surface unwarranted. Between these extreme cases are electronic events that induce a conformational change in the molecule. A typical scenario for this kind of nuclear dynamics is large displacement along one or very few vibrational modes and small displacements in the remaining modes. We have very recently had the opportunity to report on the first observation of conformational change upon inner-shell ionization. [6]

Ethanol exists in two conformations differing in internal rotational angle of the hydroxyl moiety about the CO axis. [7–10] The *anti* conformation corresponds to a dihedral HOCC angle of 180° while the *gauche* conformation has a dihedral angle of 60°. Ionization of a carbon 1s electron of the methyl carbon in the *gauche* conformation generates the ion in a state with strong Coulomb repulsion between the hydroxyl hydrogen and the now positively charged methyl group. Ionization is consequently followed by internal rotation about the carbon–carbon bond and strong excitation of the HOCC torsional mode. The relevant potential energy curves are highly anharmonic as is evident in Fig. 1. Neither an all-harmonic model nor a simple model in which the HOCC torsion is treated separately from the remaining 20 harmonic modes, are able to provide satisfactory description of the observed lineshape in the C1s photoelectron spectrum. On the other hand, a fully coupled anharmonic description of the 21 mode vibrational problem in ethanol is a truly major undertaking. Moreover, since most of the modes undergo only small displacement it may be possible to extract the correct dynamics without a fully coupled description.

Perturbation theory has proved to be the most cost-effective method to treat mechanical anharmonicity problems in small molecules [11]. Luis *et al.* conducted a perturbational study on ClO_2 to obtain a Franck-Condon profile including effects from mechanical anharmonicity [12]. However, as the size of molecule increases many states that contribute to the Franck-Condon profile tend to be degenerate or near-degenerate, and the perturbational treatment leads to unphysically large corrections to the zeroth-order wavefunctions. Matsunaga
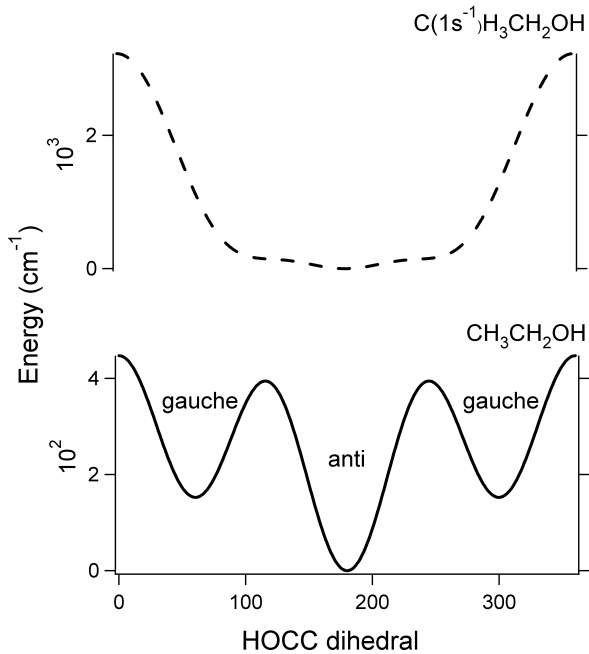
FIG. 1: Computed vibrational energy in the HOCC torsional mode, for the ground state of ethanol (solid line) and the molecule that is core-ionized at the CH_3 carbon (dashed line).

et al. developed an algorithm specifically designed for computing anharmonic vibrational states for polyatomic molecules with degeneracies occurring for excited vibrational states [13]. It is referring to as DPT2-VSCF - degenerate second order perturbational correction to vibrational self-consistent field energies. The degeneracy of states is lifted at the first order. DPT2-VSCF provides improvements over non-degenerate perturbation theory and gives results which are in very good accordance with experimental results for hydrogen peroxide and other small molecules. However, this algorithm is very time consuming for a case like ethanol, where there are hundreds of states carrying significant Franck-Condon intensity.

In this work we propose a theoretical approach for computing Franck-Condon factors in the case of a few highly excited anharmonic oscillators that are coupled to a set of weakly excited harmonic oscillators. Our approach is reminiscent of reaction path hamiltonian theory, [14] and more precisely, the basis set method advocated by Makri and Miller for describing a one-dimensional reaction coordinate coupled to a bath of many harmonic oscillators. [15] In that and later works [16, 17] the focus was on reaction kinetics or vibrational properties associated with a single electronic state, whereas here the aim is to compute Franck-Condon profiles associated with electronic transitions. The fully coupled many-dimensional vibrational problem is reduced to a (possibly large) number of low-dimensional vibrational problems that are identified in a well-defined screening process. The methodology is applied to the case of 1s ionization of methyl carbon in the *gauche* conformation of ethanol.

II. THEORY

We will be concerned with Franck-Condon theory of vibrational transitions accompanying an electronic excitation or ionization event. The formalism is well established in the case of harmonic oscillators and we will review the one-dimensional case as a way of introducing some nomenclature. Next, we extend this formalism in the spirit of the adiabatic basis set method of Makri and Miller [15], to cover the case of large geometric relaxation in a low-dimensional coordinate space, coupled to a (possibly large) set of oscillators that are intrinsically harmonic and only weakly excited.

A. The harmonic approximation

Starting from a set of internal coordinates $\mathbf{S}$, the mass-weighted normal coordinates $\mathbf{Q} - \mathbf{Q}_{eq}$ may be represented by the transformation matrix $\mathbf{L}$ as $\mathbf{S} = \mathbf{L}(\mathbf{Q} - \mathbf{Q}_{eq})$. [18] In the harmonic approximation, the many-dimensional vibrational hamiltonian decomposes into a sum of one-dimensional operators pertaining to each of the normal coordinates. A generic single-mode harmonic hamiltonian may be written

$$\hat{h} = -\frac{\hbar^2}{2}\frac{d^2}{dQ^2} + \frac{1}{2}\omega^2 Q^2, \qquad (1)$$

where ω is the angular frequency of the normal mode. Introducing a dimensionless normal coordinate q defined by $q = \gamma^{\frac{1}{2}}Q$ where $\gamma = \omega/\hbar$, the harmonic hamiltonian becomes

$$\hat{h} = \hbar^2\gamma\left(-\frac{1}{2}\frac{d^2}{dq^2} + \frac{1}{2}q^2\right) \qquad (2)$$

Normalized with respect to the mass-weighted normal coordinate Q, the corresponding stationary eigenstates may be given in terms of Hermite polynomials H_n as

$$\phi_n(q) = \left(\frac{\gamma}{\pi}\right)^{\frac{1}{4}} (2^n n!)^{-1/2} H_n(q)e^{-q^2/2} \qquad (3)$$

In the case of an electronic transition in a system with only one vibrational degree of freedom, initial- and final-state normal coordinates are related through $Q_{init} = Q - \delta Q$, where δQ denotes the initial equilibrium geometry relative to that of the final state. The probability for a monopole transition from initial-state n_{init} to final state n is given by the square of the integral

$$I_n = \int \phi_n(\gamma^{\frac{1}{2}}Q)\phi_{n_{init}}\left(\gamma_{init}^{\frac{1}{2}}(Q - \delta Q)\right) dQ \qquad (4)$$

To be specific we will take the initial vibrational state to be the ground state, $n_{init} = 0$. The Ansbacher for-

mulae [19] for Franck-Condon integrals take on a particularly simple form in terms of the ratio of angular frequencies, $\beta^2 = \omega_{init}/\omega (= \gamma_{init}/\gamma)$, and the displacement in final-state reduced coordinates, $\delta q = \gamma^{\frac{1}{2}} \delta Q$:

$$
\begin{aligned}
I_0\left[\beta, \delta q\right] &= \sqrt{\frac{2\beta}{1+\beta^2}}\, exp\left[-\frac{1}{2}\delta q^2 \frac{\beta^2}{1+\beta^2}\right] \\
I_1\left[\beta, \delta q\right] &= \delta q \frac{\beta^2}{1+\beta^2}\sqrt{2}\, I_0\left[\beta, \delta q\right] \\
I_{n>1}\left[\beta, \delta q\right] &= \delta q \frac{\beta^2}{1+\beta^2}\sqrt{\frac{2}{n}}I_{n-1}\left[\beta, \delta q\right] + \frac{1-\beta^2}{1+\beta^2}\sqrt{\frac{n-1}{n}}I_{n-2}\left[\beta, \delta q\right]
\end{aligned}
\tag{5}
$$

In the multi-dimensional case, the normal coordinates associated with two different electronic states are generally not in one-to-one correspondence but rather related by a linear transformation. This is known as the Duschinsky effect, and a large variety of methods have been devised to include it in the calculation of Franck-Condon factors. [20]

B. Coupling model

For a molecule undergoing substantial changes in geometry in the wake of an electronic transition, such as a change of conformation or dissociation of a bond, the relaxation process is likely to sample anharmonic portions of the final-state potential energy surface. While the harmonic model may not be able to give a satisfactory description of the full process, it may still be useful for most of the vibrational modes, in particular those undergoing only minor displacements. This picture suggests that the basis set method originally developed by Makri and Miller to describe a one-dimensional reaction coordinate coupled to a bath of many harmonic oscillators, [15] may be useful also to the calculation of Franck-Condon factors. The model presented below is closely related to that in Ref. [15], although it differs both with respect to the effective hamiltonian and the *Ansatz* made for the wave function. We will retain the adiabatic approximation, namely that the excitation level of each of the quasiharmonic oscillators remain good quantum numbers.

We assume a set of normal modes defined with respect to the final-state equilibrium geometry. The mass-weighted normal coordinates that describe the large amplitude relaxation from the initial-state equilibrium are collectively denoted by $\mathbf{Z}$, with the corresponding dimensionless coordinates given by $\mathbf{z}$. For simplicity, the corresponding normal modes are also referred to by $\mathbf{Z}$. The remaining set of N_{HO} oscillators are assumed to remain harmonic in the course of the electronic transition. Consistent with the preceding section, we will use symbols $\mathbf{Q}$ and $\mathbf{q}$ for these, in complete analogy to $\mathbf{Z}$ and $\mathbf{z}$. Since the $\mathbf{Z}$ modes may undergo large displacements, coupling terms to the quasiharmonic modes may be of the same order of magnitude as the harmonic potentials and should be included on an equal footing. To keep the formalism transparent, we have chosen not to take into account the Duschinsky effect, although this would be quite straight forward to do. Consistent with our neglect of the Duschinsky effect, we will omit explicit coupling between $\mathbf{Q}$ modes in the hamiltonian.

The hamiltonian describing the $\mathbf{Z}$ modes is denoted by $\hat{H}_z$ and may include any sophistication required. In our applications, we have included only mechanical anharmonicity, meaning that the kinetic energy operator is approximated by its harmonic counterpart. This is a limitation that may easily be lifted and does not limit the generality of our approach. The hamiltonian for the coupled system is chosen as

$$
\begin{aligned}
\hat{H} &= \hat{H}_z + \sum_{k=1}^{N_{HO}} \hbar^2\gamma_k\left(-\frac{1}{2}\frac{d^2}{dq_k^2} + \frac{1}{2}q_k^2 + A_k(\mathbf{z})q_k + B_k(\mathbf{z})q_k^2\right) \\
&= \hat{H}_z - \frac{1}{2}\sum_{k=1}^{N_{HO}}\hbar^2\gamma_k\frac{A_k^2}{1+2B_k} + \sum_{k=1}^{N_{HO}}\hbar^2\gamma_k\left[-\frac{1}{2}\frac{d^2}{dq_k^2} + \frac{1}{2}\left(1+2B_k\right)\left(q_k + \frac{A_k}{1+2B_k}\right)^2\right] \\
&= \hat{H}_z - \frac{1}{2}\sum_{k=1}^{N_{HO}}\hbar^2\gamma_k\frac{A_k^2}{1+2B_k} + \sum_{k=1}^{N_{HO}}\hbar^2\acute{\gamma}_k\left(-\frac{1}{2}\frac{d^2}{d\acute{q}_k^2} + \frac{1}{2}\acute{q}_k^2\right)
\end{aligned}
\tag{6}
$$

where

$$\acute{\gamma}_k = \gamma_k \left(1 + 2B_k\right)^{1/2} \qquad (7)$$

and

$$\begin{aligned}
\acute{q}_k &= (1 + 2B_k)^{1/4} \left(q_k + \frac{A_k}{1 + 2B_k} \right) \\
&= \acute{\gamma}_k^{\frac{1}{2}} \left(Q_k + \gamma_k^{-\frac{1}{2}} \frac{A_k}{1 + 2B_k} \right)
\end{aligned} \qquad (8)$$

Note that since all coordinates are assumed to be normal coordinates, A_k is of order two or higher in the $\mathbf{z}$ variables, while B_k is of order one or higher. Symmetry or numerical happenstance may shift the leading term to higher order. In accordance with our hypothesis of the N_{HO} $\mathbf{q}$ modes conducting harmonic oscillations, we will adopt the following *Ansatz* for an approximation to the wavefunction:

$$\Psi(\mathbf{z}, \acute{\mathbf{q}})_{\mathbf{n}i} = \psi_{i(\mathbf{n})}(\mathbf{z}) \prod_{k=1}^{N_{HO}} \phi_{n_k}(\acute{q}_k) \qquad (9)$$

Applying the hamiltonian to this function gives

$$\hat{H}\Psi_{\mathbf{n}i}(\mathbf{z}, \acute{\mathbf{q}}) = \left[\hat{H}_{\mathbf{0}} + \hbar^2 \sum_{k=1}^{N_{HO}} \acute{\gamma}_k n_k \right] \Psi_{\mathbf{n}i}(\mathbf{z}, \acute{\mathbf{q}}) \qquad (10)$$

where we have introduced

$$\hat{H}_{\mathbf{0}} = \hat{H}_z - \frac{1}{2}\hbar^2 \sum_{k=1}^{N_{HO}} \left(\gamma_k \frac{A_k^2}{1 + 2B_k} - \acute{\gamma}_k \right) \qquad (11)$$

Projection of eq. 10 onto the product function for the quasiharmonic modes, leads to the following equation in the anharmonic $\mathbf{z}$ degrees of freedom only:

$$\left(\hat{H}_{\mathbf{0}} + \hbar^2 \mathbf{n}^\dagger \acute{\gamma} \right) \psi_{i(\mathbf{n})}(\mathbf{z}) = E_{\mathbf{n}i}\psi_{i(\mathbf{n})}(\mathbf{z}), \qquad (12)$$

which in principle must be solved numerically for every state $(\mathbf{n}i)$ of interest. In actual applications to Franck-Condon factors, we find it necessary to retain the n_k-specific term in eq. 12, i.e. $\hbar^2 \acute{\gamma}_k n_k$, only for quasiharmonic modes that are very strongly coupled to the $\mathbf{Z}$ modes. Moreover, in this derivation, the effect of the kinetic energy operators in $\mathbf{z}$ on the $\phi_{n_k}(\acute{q}_k)$ has been omitted. To the next order of approximation, one may take into account the contribution to kinetic energy coming from the $\mathbf{z}$-dependency of A_k. Within the adiabatic approximation, this adds a term $(1/2)\hbar^2\gamma_j(dA_k/dz_j)^2(1 + 2B_k)^{-3/2}(n_k+1/2)$ to the effective potential for each pair of (q_k, z_j). In our applications this term turns out to be insignificant and will be omitted in the following.

We will be interested in computing Franck-Condon integrals between final-state solutions and the initial state given by

$$\Psi_{init}(\mathbf{z}, \mathbf{q}) = \psi_{init}(\mathbf{z}) \prod_{k=1}^{N_{HO}} \phi_{0_k}(\mathbf{q}_{init,k}) \qquad (13)$$

This notation implies the neglect of Duschinsky rotations between the two states, and, moreover, that coupling between $\mathbf{Z}$ and $\mathbf{Q}$ modes is assumed negligible in the initial state. The overlap integral reads

$$I_{\mathbf{n}i} = \int \psi_{i(\mathbf{n})}(\mathbf{z}) \left[\prod_{k=1}^{N_{HO}} \int \phi_{n_k}(\acute{q}_k)\phi_{0_k}(q_{init,k})dQ_k \right] \psi_{init}(\mathbf{z})d\mathbf{Z} \qquad (14)$$

where

$$\begin{aligned}
\int \phi_{n_k}(\acute{q}_k)\phi_{0_k}(q_{init,k})dQ_k &= \int \phi_{n_k}\left(\acute{\gamma}_k^{\frac{1}{2}}(Q_k + \gamma_k^{-\frac{1}{2}}\frac{A_k}{1+2B_k}) \right) \phi_{0_k}\left(\gamma_{init,k}^{\frac{1}{2}}Q_{init,k} \right) dQ_k \\
&= \int \phi_{n_k}\left(\acute{\gamma}_k^{\frac{1}{2}}(Q_k + \gamma_k^{-\frac{1}{2}}\frac{A_k}{1+2B_k}) \right) \phi_{0_k}\left(\gamma_{init,k}^{\frac{1}{2}}(Q_k - \delta Q_k) \right) dQ_k \\
&= \int \phi_{n_k}\left(\acute{\gamma}_k^{\frac{1}{2}}Q \right) \phi_{0_k}\left(\gamma_{init,k}^{\frac{1}{2}}(Q - \delta Q_k - \gamma_k^{-\frac{1}{2}}\frac{A_k}{1+2B_k}) \right) dQ \\
&= I_{n_k}\left[\acute{\beta}_k, \delta\acute{q}_k \right]
\end{aligned} \qquad (15)$$

where

$$\acute{\beta}_k^2 = \gamma_{init,k}/\acute{\gamma}_k = \beta_k^2(1 + 2B_k)^{-\frac{1}{2}} \qquad (16)$$

and

$$\begin{aligned}
\delta\acute{q}_k &= \acute{\gamma}_k^{\frac{1}{2}} \left[\delta Q_k + \gamma_k^{-\frac{1}{2}} \frac{A_k}{1+2B_k} \right] \\
&= (1 + 2B_k)^{\frac{1}{4}} \left[\delta q_k + \frac{A_k}{1+2B_k} \right]
\end{aligned} \qquad (17)$$

The Franck-Condon integral in eq. 14 is thus given by

$$I_{\mathbf{n}i} = \int \psi_{i(\mathbf{n})}(\mathbf{z}) \left(\prod_{k=1}^{N_{HO}} I_{n_k} \left[\acute{\beta}_k, \delta \acute{q}_k \right] \right) \psi_{init}(\mathbf{z}) d\mathbf{Z} \quad (18)$$

1. Simplifications

We consider the two-dimensional case in which there is a single z mode and a single q mode. The preceding equation 18 simplifies to

$$I_{ni} = \int \psi_{i(n)}(z) I_n \left[\acute{\beta}, \delta \acute{q} \right] \psi_{init}(z) dZ \quad (19)$$

For every state n of mode q, and every state $i(n)$ of the z mode, the Franck-Condon intensity for transition to the two-mode state (n,i) is given as the square of I_{ni}. The total energy of this state is given by eigenvalue E_{ni} as it appears in eq. 12.

Assume now that $\acute{\gamma}$ varies only insignificantly with z. This allows us to treat the term $\hbar^2 n \acute{\gamma}$ as a constant in eq. 12, in which case the solutions of eq. 12 are independent of n and may be labeled by i alone. Moreover, if the $\hbar^2 n \acute{\gamma}$ term is dropped from the hamiltonian altogether, the z energy levels are independent of i. In this case, the total energy of the two-mode state (n,i) is obtained as $E_i + \hbar^2 n \acute{\gamma}$ and the corresponding Franck-Condon intensities may be computed from a single set of $\psi_i(z)$ functions for all n. Finally, if $I_n \left[\acute{\beta}, \delta \acute{q} \right]$ varies only slowly with z in the sampled region, the integral may be factorized into q and z contributions. Similar considerations are useful also in the many-dimensional case as summarized in Fig. 2. Following the flowchart, all quasinormal modes that are vibrationally excited may be classified into four groups, characterized by whether or not their harmonic frequency and/or Franck-Condon integrals vary with $\mathbf{z}$. This opens for well justified simplifications of the working equations in each case.

III. COMPUTATIONAL DETAILS

A. Electronic and geometric structures

The electronic structure calculations were conducted using three different levels of theory, all in conjunction with Dunning triple-ζ basis sets augmented with 6-311G(d,p) polarization functions [21, 22]. Some tests were carried out with the more elaborate aug-cc-pVTZ basis set, but at the B3LYP level of theory differences between the results obtained with the two basis sets were inconsequential to our study.

The hybrid density functional method B3LYP was used as implemented [23] in the Gaussian-03 set of programs [24] for computing harmonic frequencies and normal coordinates for neutral and C1s-ionized ethanol as well as anharmonic corrections including the mode-coupling potential. The numerical integration was carried out on an ultrafine grid. For the ionized species, the core hole was described by an effective core potential [25, 26].

Franck-Condon factors are particularly sensitive to changes in geometries that occur during ionization, and we found that the geometry changes computed by means of B3LYP were too inaccurate for use in the present study of mode-coupling effects. Hence, the neutral and C1s-ionized species were reoptimized in their *anti* conformation using a highly accurate *ab initio* approach; Coupled-Cluster with Single and Double excitations and including a perturbational estimate of the contribution from Triple excitations [CCSD(T)]. For the *gauche* conformations which belongs to the C_1 point group, these calculations were not feasible. Rather, corrections to bond lengths and angles were obtained as differences between B3LYP and CCSD(T) values as obtained for the *anti* conformation. While these calculations used an ECP approach to describe the ionized core, we found that there are minor yet in the present context, significant differences between calculations in which the core hole is treated explicitly (Hole-State calculations; HSC) and those in which it is simulated by the effective core potential (ECP). For a corrected geometry, G, of the core-ionized state, we assume that the corrections are additive and write

$$G_{corr} = G_{CCSD(T)}^{ECP} - (G_{RHF}^{HSC} - G_{RHF}^{ECP}) \quad (20)$$

The principal result of this correction is to decrease the predicted contraction of the C–C bond (by 0.15 pm and 0.18 for *anti*- and *gauche*-ethanol,) and C–O bonds (by 0.26 pm for both conformations).

B. Computing mode-coupling terms: $\mathbf{A}_k(z_1)$ and $\mathbf{B}_k(z_1)$

The nomenclature used here is introduced in sec. II. In order to evaluate coupling coefficients between mode z_1 and mode q_k, say, we have used a finite-difference approach in normal coordinates. Starting from the *anti*-conformation (the lowest energy structure of ethanol ionized at the CH_3 carbon), the $\mathbf{L}$ matrix is computed according to Ref. [27]. The change in symmetry coordinates induced by a displacement δq_k is given by the product of $\delta q_k, \gamma_k^{-1/2}$ and the associated column vector in L. This true also for z_1, and the total displacement in symmetry coordinates is added to the starting geometry to define the modified geometry. The energy $E(z_1, \delta q_k)$ is computed for each modified geometry, and the energy contribution due to mode coupling, $W(z_1, \delta q_k)$, may be identified as

$$W(z_1, \delta q_k) = E(z_1, \delta q_k) + E(0,0) \\ - E(0, \delta q_k) - E(z_1, 0) \quad (21)$$
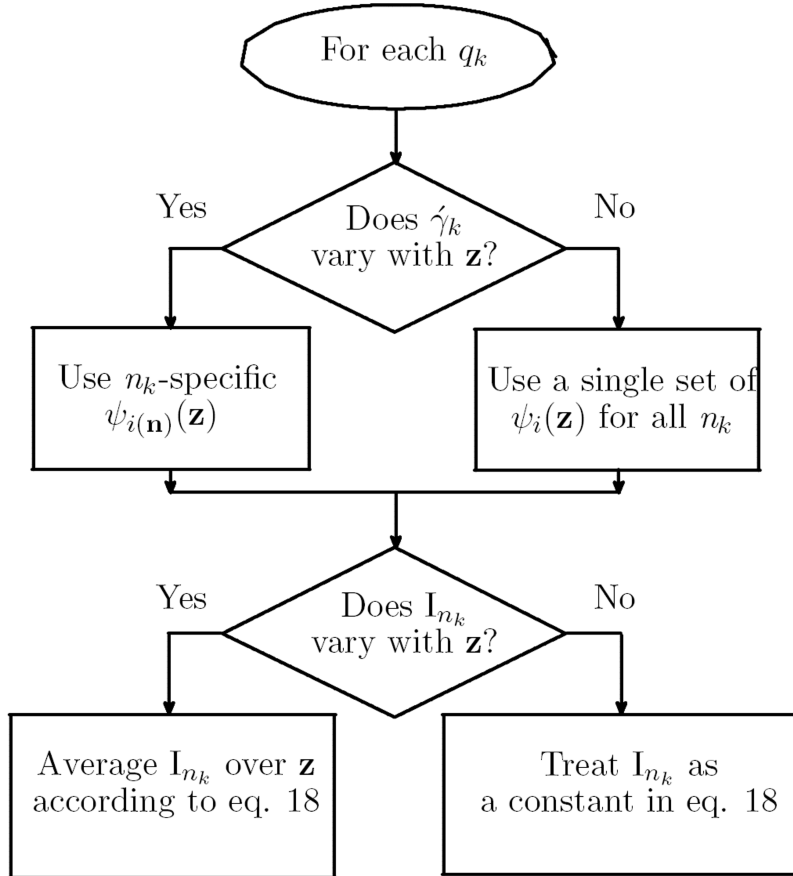
FIG. 2: Scheme for analyzing the coupling contribution from each individual quasinormal mode.

The coupling form, when truncated at the second order, reads

$$W(z_1, \delta q_k) = \left[A_k(z_1)\delta q_k + B_k(z_1)\delta q_k^2 \right] \hbar^2 \gamma_k \qquad (22)$$

It may be noticed that the terms between the square brackets are dimensionless. To determine $A_k(z_1)$ and $B_k(z_1)$ terms, a minimum of two distortions along the q_k coordinate is needed for every value of z_1. Using symmetric distortions, i.e. $\pm\delta q_k$, one obtains expressions that are correct to $O(\delta q_k^3)$ for A_k and $O(\delta q_k^4)$ for B_k:

$$A_k(z_1) = \frac{W(z_1, +\delta q_k) - W(z_1, -\delta q_k)}{2\hbar^2 \gamma_k \delta q_k} \qquad (23)$$

and

$$B_k(z_1) = \frac{W(z_1, +\delta q_k) + W(z_1, -\delta q_k)}{2\hbar^2 \gamma_k \delta q_k^2} \qquad (24)$$

The resulting functions were checked against those obtained from difference formulae correct to two orders higher than those just quoted. The z_1 dependency of the A and B coefficients were mapped out on an equidistant grid with step size 0.45 (corresponding to steps of 0.2 amu$^{1/2}$Å in Z_1).

C. Lineshape models

To each site of ionization and conformation, a set of Franck-Condon factors are computed and transformed into a continuous lineshape model by convolution with broadening functions that reflect the natural linewidth, Gaussian resolution, and the interaction between the photoelectron and the Auger electron emitted in the de-excitation of the core-hole state. The latter interaction is described using Eq.(12) from van der Straten *et al.* [28]. The four resultant lineshapes (one for each different core-ionized carbon) are fit by least-squares techniques [29] to the experimental data with the adiabatic energy position of each profile, three independent intensity parameters as well as a constant background as fitting parameters.

IV. APPLICATION TO ETHANOL

In this section we apply the proposed coupling model to the case of C1s photoionization of *gauche* ethanol in its vibrational ground state. As described in the *Introduction*, 1s ionization of the methyl carbon takes the

molecule to a potential energy surface (PES) for which the *gauche* structure is no longer an equilibrium point. The molecule subsequently undergoes large relaxation in the HOCC torsional angle. Formally, the adiabatic transition corresponds to a change from *gauche* to the *anti* conformation, although a vanishing FC factor dictates that this transition is not seen in the photoelectron spectrum.

The normal coordinate corresponding to HOCC torsion is strongly anharmonic and undergoes a large displacement and is labeled Z_1 according to the nomenclature introduced in the preceding section. The remaining normal coordinates change considerably less and coupling between Z_1 and the other normal coordinates is, with one exception, well represented by the model defined in eq. 6. The exception is internal rotation of the methyl moiety, for which we find it necessary to include coupling to Z_1 in a bivariate power expansion up through fifth order in both coordinates. To facilitate this within the present formalism, we include the methyl rotation coordinate as Z_2, although we will not compute explicit coupling terms between Z_2 and the remaining 19 pseudoharmonic normal coordinates. The one-dimensional final-state potentials are expressed as polynomials of order six in z_1 and second order in z_2. The (z_1, z_2)-eigenproblem in eq. 12 is solved in a product basis of harmonic oscillator functions, of dimension 15×10.
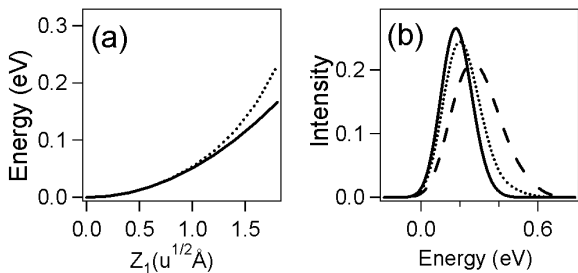

FIG. 3: (a) Left: Torsional potential along the HOCC(z_1) coordinate in the final state, in the harmonic approximation (full line) and including terms of higher order in z_1 (dotted); Right: Two-dimensional Franck-Condon profiles in (z_1, z_2), in the harmonc approximation (dotted), including single-mode anharmonic terms (full line) and including both single-mode and mode-coupling anharmonic terms (dashed).

Fig. 3(a) shows the final-state torsional potential in the z_1 coordinate, with and without anharmonic corrections. The anharmonic terms in the z_1 potential makes the torsion about the C–O bond stiffer, and the net effect is to broaden the associated Franck-Condon profile and shift it to higher energy, cf Fig. 3(b). Inclusion of coupling to z_2 has an even larger impact on the FC profile, acting in the same direction as the described for the unimode anharmonicity.

In order to take into account coupling between z_1 and the 19 quasinormal coordinates, the latter are classified according to the algorithm laid out in Fig. 2. First,
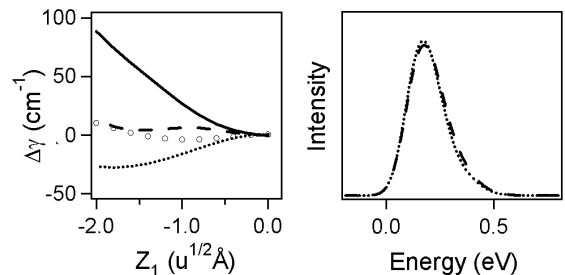

FIG. 4: (a) Left: Variation in the harmonic frequency due to coupling to the HOCC (z_1) coordinate of four modes; Q_1 (CCO bending, solid line), Q_2 (COH+CCH bending dotted line), Q_3 (CO stretching, dashed), and Q_4 (CC stretching, circles). (b) Right: Two-dimensional Franck-Condon profiles in the (z_1, q_1) coordinates, differing in whether (dotted line) or not (dashed line) the effective z_1 potential in eq. 12 includes the excitation level of the Q_1 mode.

the variation in harmonic frequency is mapped out as a function of z_1, cf. Fig. 4(a). Only for two of the Q-modes, the CCO bending mode (Q_1) and a mode involving CCH and COH bending (Q_2), does the vibrational frequency change appreciably over a range of 2.0 $u^{\frac{1}{2}}$Å in Z_1, and more so for Q_1 than Q_2 (80 cm^{-1} *vs* 30 cm^{-1}). Only for the first of the two does inclusion of n_1-specific terms in the effective (z_1, z_2) hamiltonian in eq. 12 lead to discernible changes in the Franck-Condon profile, cf. Fig. 4(b). Even in this case the impact is very modest.

Next, we explore how the one-dimensional Franck-Condon factors for the quasiharmonic modes vary with z_1 as a result of coupling terms. For each mode, the dependency on z_1 is conveniently represented by the so-called *S factor*, found as the ratio between I_1 and I_0 in eqns. 5. This quantity is shown in Fig. 5 as a function of z_1 for the four modes for which it varies the most. While the S factors for two of the bending modes (Q_1 and Q_2) vary significantly with Z_1, the change is much less for the C–O stretching mode (Q_3) and negligible for C–C stretching (Q_4). To illustrate how this translates into Franck-Condon profiles, Fig. 6 shows the two-dimensional FC profiles as z_1-dependent integrals lead to FC profiles which differ significantly from those obtained using equilibrium geometries, i.e. at a single value of z_1. For both Q_1 and Q_2, the mean vibrational energy shifts to lower energy and the width of the FC envelope decreases. This can be understood from Fig. 5 since the S factor drops as one departs from $z_1 = 0$.

From the preceding discussion, one may conclude that for four normal modes, coupling to the HOCC torsional mode may have significant impact on the Franck-Condon lineshape associated with carbon 1s ionization of the methyl moiety in *gauche* ethanol. The interacting modes include methyl rotation and three quasiharmonic normal modes (CCO, Q_2, CO), in addition to HOCC torsion. The remaining 16 modes show negligible coupling to the HOCC modes and are treated as uncoupled oscillators,
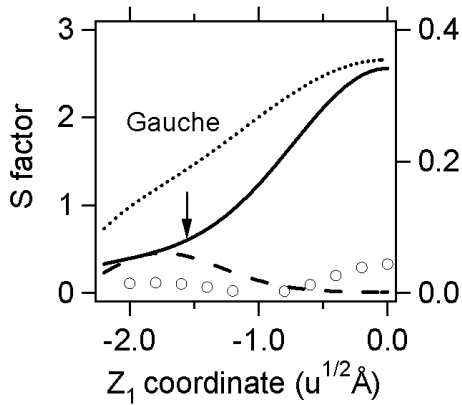
FIG. 5: Z_1-dependent S factor of the CCO mode (solid line), Q_2 (dotted line), the C–O mode (dashed line), and the C–C mode (circles). The *anti* geometry is taken as a reference point.
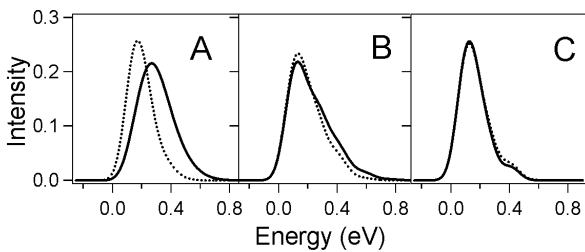

FIG. 6: Effect of using z_1-dependent integrals on the 2-mode FC envelope of (A) HOCC-CCO model, (B) HOCC-Q_2 model, and (C) HOCC-CO model. The solid line represents the harmonic FC integrals, i.e. integrals evaluated at $z_1=0$, while the dotted line is obtained according to eq. 19.

either Morse (symmetric CH$_3$ stretching) or harmonic oscillators (15 modes). The Franck-Condon (FC) profile obtained on the basis of the five coupled modes is subsequently convoluted with FC factors for the remaining 16 modes. The effect of mode coupling on the total FC profile is shown in Fig. 7, where the main effect is seen to be a shift toward lower mean vibrational energy and reduction in linewidth. There are also changes to the shape of the profile.

A.   Theory vs experiment

The experimental carbon 1s photoelectron spectrum of gas-phase ethanol as obtained under conditions described in Ref. [6], is shown as circles in Fig. 8. It consists of two main peaks, corresponding to ionization of the methyl carbon (left, at low energy) and the functionalized carbon (right, at high ionization energy). Both structures receive contributions from both the *gauche* and *anti* conformations of ethanol. In order to model the spectrum one needs FC envelopes pertaining to each of the two
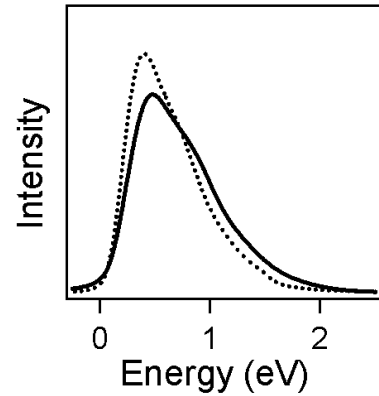

FIG. 7: Vibrational envelope associated with C1s ionization of the methyl end of *gauche* ethanol. The solid line corresponds to a model of uncoupled oscillators, whereas the dotted line corresponds the coupling model outlined in the text.

conformations as well as the two sites of ionization, i.e. four contributions. Only ionization of the methyl moiety and in the *gauche* conformation of ethanol, leads to large geometric relaxation to the extent that a coupled-mode treatment is required. This leads to the FC profile shown in Fig. 7, which may be combined with FC profiles based on the harmonic oscillator approximation for C1s ionization of *anti*-ethanol and for ionization of the functionalized carbon in *gauche* ethanol, cf the appendix for details.

The resulting model spectrum is fit in the least-squares sense to the experimental spectrum by taking the *anti*-to-*gauche* intensity ratio and the adiabatic energy positions as fitting parameters. The best fit is obtained when the *anti*-to-*gauche* ratio is around 0.41:0.59, cf the full drawn line in Fig. 8. This number may be compared to the relative populations of 62% and 38% of *gauche*- and *anti*-conformations, respectively, as obtained by Pearson *et al.* [30]. The agreement between theory and experiment is very satisfying, cf the leftmost main structure in Fig. 8. More than reproducing the overall lineshape, details like the low-energy shoulder of the spectrum and the flattening on the high-energy side of the methyl peak are satisfactorily accounted for.

V.   CONCLUSIONS

A model has been presented for computing Franck-Condon factors for systems which undergoes large geometric changes in only a few normal coordinates. The model reduces the anharmonic oscillator problem to a few-body problem, albeit with corrections due to coupling to harmonic modes. The approach works very well for core-ionization of ethanol.
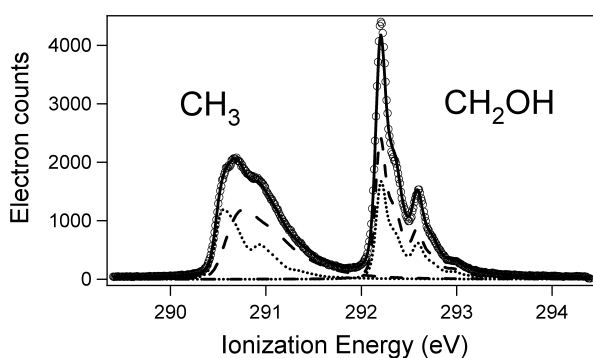
FIG. 8: Experimental (circles) and theoretical (solid line) carbon 1s photoelectron spectrum of ethanol. The individual contributions from the *anti* (dotted lines) and *gauche* (dashed lines) conformations are also shown.

[1] P. Chen, *Unimolecular and Bimolecular Dynamics* (John Wiley and Sons, 1994), chap. 8, pp. 372–425.

[2] T. Karlsen, L. J. Sæthre, K. J. Børve, N. Berrah, E. Kukk, J. D. Bozek, T. X. Carroll, and T. D. Thomas, J. Phys. Chem. A **105**, 7700 (2001).

[3] S. Sundin, L. J. Sæthre, S. Sorensen, A. Ausmeees, and S. Svensson, J. Chem. Phys. **110**, 5806 (1999).

[4] S. J. Osborne, S. Sundin, A. Ausmeees, S. Svensson, L. J. Sæthre, O. Sværen, S. Sorensen, J. Vgh, J. Karvonen, S. Aksela, et al., J. Chem. Phys. **106**, 1661 (1997).

[5] K. J. Børve, L. J. Sæthre, T. D. Thomas, T. X. Carroll, N. Berrah, J. D. Bozek, and E. Kukk, Phys. Rev. A **63**, 012506 (2001).

[6] M. Abu-samha, K. J. Børve, L. J. Sæthre, and T. D. Thomas, Phys. Rev. Lett. **95**, 103002 (2005).

[7] H. L. Fang and R. L. Swofford, Chem. Phys. Lett. **105**, 5 (1984).

[8] R. A. Shaw, H. Wieser, R. Dutler, and A. Rauk, J. Am. Chem. Soc. **112**, 5401 (1990).

[9] D. Schiel and W. Richter, J. Chem. Phys. **78**, 6559 (1983).

[10] J. M. Jasinski, Chem. Phys. Lett. **109**, 462 (1984).

[11] P. W. Atkins and R. S. Friedman, *Molecular Quantum Mechanics* (Oxford University Press, 2001).

[12] J. M. Luis, D. M. Bishop, and B. Kirtman, J. Chem. Phys. **120**, 813 (2004).

[13] N. Matsunaga, G. M. Chaban, and R. B. Gerber, J. Chem. Phys. **117**, 3541 (2002).

[14] W. H. Miller, N. C. Handy, and J. E. Adams, J. Chem. Phys. **72**, 99 (1980).

[15] N. Makri and W. H. Miller, J. Chem. Phys. **86**, 1451 (1987).

[16] V. A. Benderskii, E. V. Vetoshkin, I. S. Irgibaeva, and H. P. Trommsdorff, Chem. Phys. **262**, 393 (2000).

[17] D. Lauvergnat and A. Nauts, Chem. Phys. **305**, 105 (2004).

[18] J. E. Bright Wilson, J. C. Decius, and P. C. Cross, *Molecular vibrations* (Dover, 1980), chap. 2.5.

[19] F. Ansbacher, Z. Naturforschg. **14a**, 889 (1959).

[20] A. Toniolo and M. Persico, J. Comput. Chem. **22**, 968 (2001).

[21] T. H. Dunning, Jr., J. Chem. Phys. **55**, 716 (1971).

[22] R. Krishnan, J. S. Binkley, R. Seeger, and J. A. Pople, J. Chem. Phys. **72**, 650 (1980).

[23] P. J. Stephens, F. J. Devlin, C. F. Chabalowski, and M. J. Frisch, J. Phys. Chem. **98**, 11623 (1994).

[24] M. J. Frisch, G. W. Trucks, H. B. Schlegel, G. E. Scuseria, M. A. Robb, J. R. Cheeseman, J. A. Montgomery, Jr., T. Vreven, K. N. Kudin, J. C. Burant, et al., *Gaussian 03, Revision C*, Gaussian, Inc., Wallingford, CT, 2004.

[25] W. J. Stevens, H. Basch, and M. Krauss, J. Chem. Phys. **81**, 6026 (1984).

[26] T. Karlsen and K. J. Børve, J. Chem. Phys. **112**, 7979 (2000).

[27] L. Hedberg and I. M. Mills, J. Molec. Spectrosc. **160**, 117 (1993).

[28] P. van der Straten, R. Morgenstern, and A. Niehaus, Z. Phys. D **8**, 35 (1988).

[29] E. Kukk, *SPANCF (2000)* - `http://www.geocities.com/ekukk` (2000).

[30] J. C. Pearson, K. V. L. N. Sastry, E. Herbst, and F. C. DeLucia, J. Molec. Spectrosc. **175**, 246 (1996).

[31] L. J. Sæthre, O. Sværen, S. Svensson, S. Osborne, T. D. Thomas, J. Jauhiainen, and S. Aksela, Phys. Rev. A **55**, 2748 (1997).

[32] V. M. Oltedal, K. J. Børve, L. J. Sæthre, T. D. Thomas, J. D. Bozek, and E. Kukk, Phys. Chem. Chem. Phys. **6**, 4254 (2004).

TABLE I: Geometry change upon C1s ionization in *anti*- and *gauche* conformers of ethanol. Bond length changes in *pm* and angles in degrees.

| | C*H$_2$OH | | C*H$_3$ | |
Coordinate	*anti*	*gauche*	*anti*	*gauche*
C-C	-0.49	-1.55	0.75	0.03
C-O	-3.11	-2.91	-4.44	-4.21
O-H	1.12	1.09	0.45	0.41
C$_2$H(t)	-0.38	-0.37	-5.63	-5.72
C$_1$H	-5.67	-5.34	-0.33	-0.01
C$_2$H	-0.41	-0.44	-5.32	-5.43
CCO	0.24	2.34	-4.90	-9.76
HOC	-0.53	-0.87	2.57	2.95
H(t)C$_2$C$_1$	-2.07	-2.14	1.74	1.58

APPENDIX A: FC ANALYSIS OF THE REMAINING CARBON SITES

The fact that ethanol offers two inequivalent carbon sites and also exists in two different conformations, implies that there are altogether four different contributions to the C1s photoelectron spectrum of this molecule. Only the methyl carbon in the *gauche* conformer gives rise to large structural relaxation following C1s ioniza-

tion. For the remaining three combinations, we prepare C1s lineshape models in the harmonic approximation. This involves calculation of the equilibrium geometries and normal modes for the neutral and core-ionized molecules [31, 32], cf the geometry changes upon core-ionizing as shown in Tab. A. Core-ionizing the functionalized carbon leads to almost identical vibrational structures for the two conformations, see Fig. 8. The vibrational structure consists of a shoulder at around 150 meV higher energy than the main peak, corresponding to excitation of the C–O and C–C stretching modes and the CCH bending mode. The first excited state of the C*–H stretching mode gives rise to a satellite at 420 meV above the adiabate.

If we consider ionization of the methyl moiety in the *anti* conformation of ethanol, the ionization event is accompanied by vibrational excitations of the CCO bending mode at 58 and 116 meV vibrational energy and with intensities of 72% ($\nu = 1$) and 28%($\nu = 2$) of the main peak. Additional singly excited states in C–C and C–O stretching modes and the CCH bending mode contribute to a broad main peak. The satellite at 420 meV is due to the singly excited state of the C*–H stretching mode.